CENTRAL RESEARCH LIBRARY
DOCUMENT COLLECTION

OAK RIDGE NATIONAL LABORATORY
OPERATED BY
UNION CARBIDE CORPORATION
NUCLEAR DIVISION

POST OFFICE BOX X
OAK RIDGE, TENNESSEE 37830

ORNL-MIT- 129

DATE: April 28, 1971

COPY NO. 16

SUBJECT: Adsorption and Filtration of Trace Contaminants in Aqueous Effluents

AUTHOR: M.M. Irizarry and D.B. Anthony

Consultant: Fred Nelson

ABSTRACT

The removal of trace copper contaminants from aqueous effluents by means of adsorption on ion exchange resins has been studied. A semi-continuous, axial filtration device was used to obtain mass transfer data as a function of the operating parameters: flow rate, resin volume and size, temperature, rotational speed, and system geometry. Correlation of data based on power dissipation per unit volume is presented. Operation of the unit involved high product fluxes (1000 - 15,000 gpd/ft^2) and adsorption efficiencies (90 - 99+%) coupled with low pressure drops (0 - 10 psi).

OAK RIDGE NATIONAL LABORATORY
CENTRAL RESEARCH LIBRARY
DOCUMENT COLLECTION
LIBRARY LOAN COPY
DO NOT TRANSFER TO ANOTHER PERSON
If you wish someone else to see this document, send in name with document and the library will arrange a loan.
UCN-7969
(3 3-67)

Oak Ridge Station
School of Chemical Engineering Practice
Massachusetts Institute of Technology

This report was prepared as an account of work sponsored by the United States Government. Neither the United States nor any of its employees, nor any of its contractors, subcontractors, or their employees, makes any warranty, express or implied, or assumes any legal liability or responsibility for the accuracy, completeness or usefulness of any information, apparatus, product or process disclosed, or represents that its use would not infringe privately owned rights.

Contents

	Page
1. Summary	4
2. Introduction	5
2.1 Background	5
2.2 Objectives and Method of Attack	5
3. Apparatus and Procedure	6
3.1 Description of Apparatus	6
3.2 Materials and Experimental Concentrations	6
3.3 Procedure	6
3.4 Radiometric Analytical Technique	9
4. Theoretical Considerations and Previous Work	9
4.1 Ion Exchange Phenomena	9
4.2 Material Balance	10
4.3 Mass Transfer Correlations	11
5. Results and Discussion of Results	12
5.1 Effect of Flow Rate	12
5.2 Effect of Resin Volume	14
5.3 Effect of Resin Diameter	14
5.4 Effect of Temperature	18
5.5 Effect of Rotational Speed and Annular Gap Width	18
5.6 Use of Genralized Correlation	22
5.7 Large-Scale Implications	22
6. Conclusions	24
7. Recommendations	25
8. Acknowledgements	25
9. Appendix	26
9.1 Sample Calculations	26
9.2 Alternate Derivation for Mass Transfer Expression	34
9.3 Theoretical Model for Particle Interactions	35
9.4 Procedure for Experimental Power Measurements	35
9.5 Temperature Dependence of Generalized Correlation	36
9.6 Error Analysis	37
9.7 Summary of Data and Calculated Values	39
9.8 Location of Original Data	39
9.9 Nomenclature	39
9.10 Literature References	43

1. SUMMARY

An axial filtration apparatus has been investigated for the adsorption of tracer copper from aqueous solutions. Experimental operation of the system involved continuous introduction of a contaminated stream into the annular space between two concentric cylinders where it was contacted by a well-mixed ion exchange resin suspension. Fluid motion was induced by rotation of the inner cylinder which was fitted with a stainless steel filter. Radiometric techniques were used to monitor copper concentrations.

The mass transfer phenomena were studied as a function of several operating parameters: flow rate (100 - 1500 ml/min), resin volume (1 - 32 vol %), particle size (50 - 400 mesh), temperature (25 - 55°C), rotational speed (600 - 6000 rpm), and annular cell size (185 - 3000 ml). Pursuant to this investigation a literature search was conducted to review the correlations for mass transfer to suspended particles in agitated vessels.

The primary findings of the study were:

1. Successful attainment of high product flux (1000 - 15,000 gpd/ft^2) and adsorption efficiencies (90 - 99+%) with low pressure drops (0 - 10 psi).

2. A material balance based on a first order mass transfer approximation yielded the following expression, valid for high adsorption levels and distribution coefficients and low resin loadings.

$$\frac{C}{C_o} \cong \frac{\overline{R}\,F}{3k\overline{V}} \qquad (1)$$

C_o and C are fluid phase copper concentrations entering and leaving the system, $\overline{R}$ is the mean particle radius, F is the volumetric flow rate, $\overline{V}$ is the resin volume, and k is the overall mass transfer coefficient.

3. The mass transfer coefficient is well-described for the region of study by the correlation of Brian, Hales, and Sherwood (3).

$$N_{Sh} = a\left[\frac{P}{V}\,\frac{d^2\,\rho_L^2}{\mu_L^3}\right]^{n/3} N_{Sc}^{1/3} \qquad (2)$$

For a = 0.87 and n = 0.40, where N_{Sh} is the Sherwood number, N_{Sc} is the Schmidt number and P/V is the power per unit fluid volume with d being the particle diameter. This correlation, however, is not valid for high resin contents (volume percent greater than 20) and high resin loadings.

4. The dependence of the mass transfer coefficient on temperature was found in terms of an activation energy, 6 kcal/gmole.

The major recommendations include further study on the effect of particle concentration, development of in situ regeneration techniques, and adaptation of the unit to provide more efficient mixing.

2. INTRODUCTION

2.1 Background

As stated in a recent technical journal, "removing even trace quantities of metals that are suspected of having a bad effect on the environment, or of being toxic to humans, is becoming an increasingly important industrial problem" (28). The article further identifies adsorption techniques as critical to the solution of the problem.

A laboratory-scale filtration device has been constructed by the Water Research Group of Oak Ridge National Laboratory for investigation of the removal of trace contaminants from aqueous effluents. The device incorporates the adsorption of contaminants on a substrate and cross-flow filtration in a single unit. Semicontinuous operation is possible allowing for in situ regeneration. The device has been successfully employed to remove trace metal ions such as copper (II), arsenic (V), and mercury (II). Rejections greater than 99% and product flux rates over 3000 gpd/ft^2 at a differential pressure of 8 psi were successfully achieved (17). This process offers several possible advantages over mixer settler contactors, fixed bed or fluidized bed operations: low pressure drops, no carryover of adsorbent in the affluent, and good mixing.

2.2 Objectives and Method of Attack

The objective of this work was to develop a better understanding of the operational behavior of the axial filtration device. Primary efforts were directed toward determining a generalized correlation for scaleup and subsequent economic analysis.

The problem was approached through a basic mass transfer study with particular emphasis on applicable models. Specific questions of interest were:

1. Accuracy of radiometric analytical techniques for copper concentrations of 10^{-8} M. Verification of the precision of this method was undertaken at the outset of the project.

2. Effect of operating variables. Such parameters included flow rate, amount of resin used, particle size, temperature, mixing parameters, and system geometry.

3. Validity of available theoretical and empirical correlations. The impetus was to permit accurate prediction of system performance over a wide range of conditions and scaleup for large scale operations.

3. APPARATUS AND PROCEDURE

3.1 Description of Apparatus

The axial filtration unit, as shown in Fig. 1, consisted of a cylindrical vessel and concentric cylindrical rotor fitted with a stainless steel filter. The cell was charged with adsorbent. Liquid was fed under a slight pressure while the inner cylinder was rotated. The liquid permeated radially inward through the filter and was collected axially from the hollow center of the shaft. Three annular gap widths, b, were studied (0.85, 1.52, and 6.12 cm).

The complete experimental flow system is illustrated in Fig. 2. Process water was monitored with a rotameter to maintain the desired inlet feed rate. Contaminant solution, containing a small amount of radioactive Cu^{++} tracer, was injected into the primary flow system by a Pall metering syringe pump. After passing through the filtration device, the effluent was discharged to a 'hot drain' (designated specifically for radioactive wastes). The system was operated continuously with interruption only for replacement of adsorbent. Temperature control ($\pm$ 2°C) was obtained with a heating bath and a "Porta-Temp" controller.

3.2 Materials and Experimental Concentrations

The adsorbent used was a Dowex 50W-X12 cation exchange resin, a typical sulfonated polystyrene resin with 12% divinylbenzene crosslinking. Capacity calculations are included in Appendix 9.1.1. Three adsorbent sizes were used: dry basis, 50-100, 100-200, and 200-400 U.S. Standard mesh. The volume of resin quoted in the report is wet volume corrected for the void fraction (see Appendix 9.1.1).

The contaminant reservoir contained a prepared aqueous solution of $Cu(NO_3)_2$(4×10^{-4} M) and HNO_3(0.10 M). A small amount of radioactive $Cu(NO_3)_2$ solution was added as a tracer. The feed water to contaminant dilution ratio was 100:1, thereby providing inlet concentrations of Cu^{++} and HNO_3 of 4×10^{-6} M and 10^{-3} M, respectively.

3.3 Procedure

The annular space was filled with a measured quantity of resin. Process flow was started and the temperature controller set-point was manually

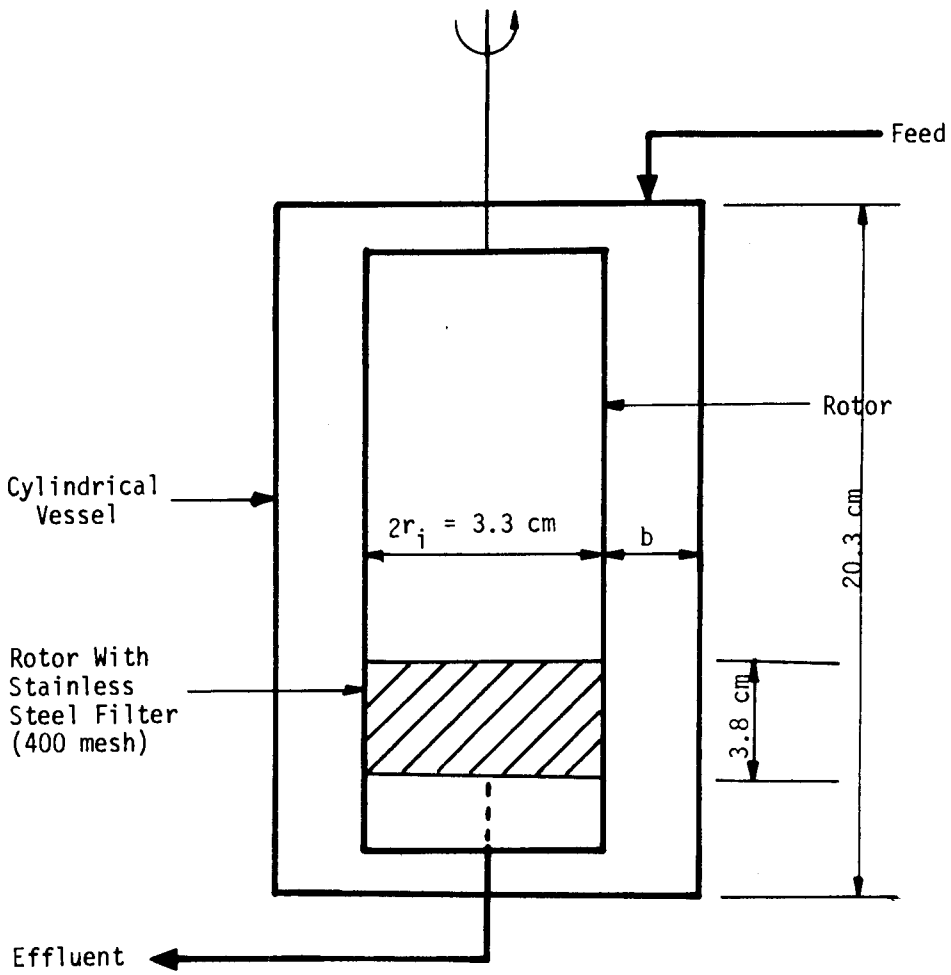

b = annular gap width

MASSACHUSETTS INSTITUTE OF TECHNOLOGY SCHOOL OF CHEMICAL ENGINEERING PRACTICE AT OAK RIDGE NATIONAL LABORATORY			
AXIAL FILTRATION UNIT			
DATE 4-15-71	DRAWN BY MI	FILE NO. CEPS-X-129	FIG. 1

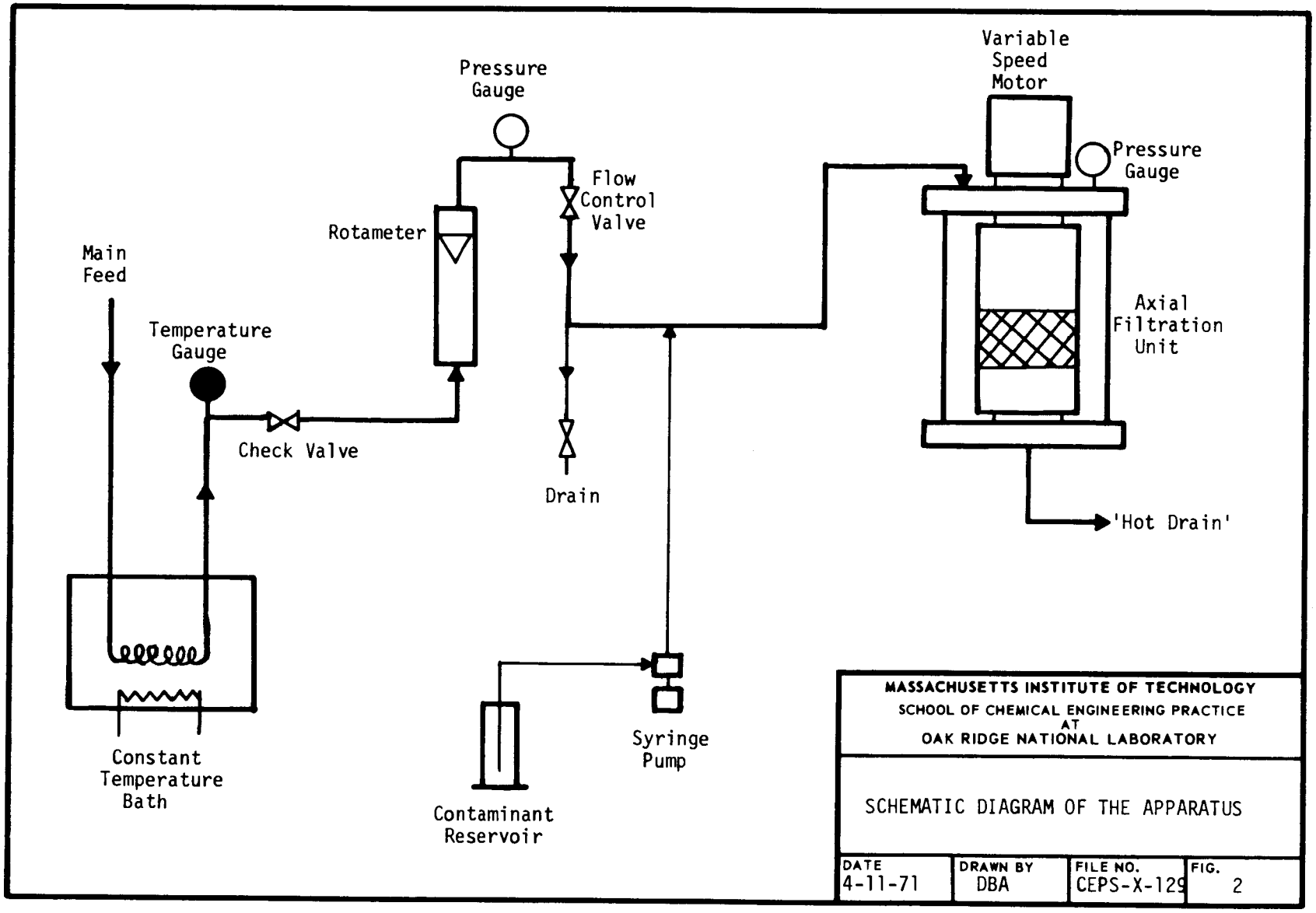
Pressure Gauge
Variable Speed Motor
Pressure Gauge
Flow Control Valve
Rotameter
Main Feed
Temperature Gauge
Axial Filtration Unit
Check Valve
Drain
'Hot Drain'
Constant Temperature Bath
Syringe Pump
Contaminant Reservoir
MASSACHUSETTS INSTITUTE OF TECHNOLOGY
SCHOOL OF CHEMICAL ENGINEERING PRACTICE
AT
OAK RIDGE NATIONAL LABORATORY
SCHEMATIC DIAGRAM OF THE APPARATUS
DATE 4-11-71
DRAWN BY DBA
FILE NO. CEPS-X-129
FIG. 2

adjusted to the desired level. The rotor was started, and then the primary flow was set at the prescribed rate. The syringe pump and timer were simultaneously started. After steady state operation was obtained, 500-ml samples were collected from the effluent stream. The time of collection was noted.

3.4 Radiometric Analytical Technique

Radioactive copper (II) tracer was used to monitor concentrations. Tracer samples were prepared by irradiating a 10-mg sample of $Cu(NO_3)_2$ in the ORNL Research Reactor for 8-10 min (activity calculations are given in Appendix 9.1.2). ^{64}Cu has a half life of 12.9 hr making each sample good for two days of experimentation ($\sim$4 half lives).

To permit accurate analysis of effluent copper concentrations (as low as 10^{-8} M), the copper content of the 500-ml sample was concentrated on 2 cc of 200-400 mesh Dowex-50 resin for a set time period. It was determined experimentally that 30 min resulted in 99.8% adsorption of the copper on the resin. The activity of the concentrated sample was measured in a RIDL Counter Model 49-43 and compared with a measured sample of contaminant solution. Subsequent calculations for experimental evaluation are detailed in Appendix 9.1.3.

4. THEORETICAL CONSIDERATIONS AND PREVIOUS WORK

4.1 Ion Exchange Phenomena

From a mass transfer standpoint the rate determining step in ion exchange is the interdiffusion of counter ions. This step may be limited by diffusion through a fluid film at the surface of the resin, by diffusion within the bead structure itself, or a combination of the two. Film diffusion (liquid phase limiting) is characterized by a strong dependence on solution concentration and distribution coefficient of the adsorbed species, fluid transport properties, and the hydrodynamic nature of the system. Selke and Bliss (22) indicate a liquid diffusion controlled process for the ion exchange of copper in a fixed bed. This model is particularly applicable when resin loading is low and the distribution coefficient is high. Diffusion through a thin stagnant film, of thickness δ, may be expressed as:

$$- V \frac{dC}{dt} = \frac{\mathcal{D}}{\delta} \overline{A}(C - C_e) \qquad (3)$$

where C and C_e are liquid phase concentrations in the bulk solution and at the resin surface, t = time, $\mathcal{D}$ = diffusion coefficient, V = fluid volume, and $\overline{A}$ = surface area. Equilibrium considerations (detailed in Appendix

9.1.4) indicate that for excess resin capacity the fluid concentration at the surface is effectively zero. Coupling this with a definition of the overall mass transfer coefficient, one obtains

$$k = \frac{\mathcal{D}}{\delta} \tag{4}$$

where k is a first order mass transfer coefficient defined by the equation

$$- V \frac{dC}{dt} = k\overline{A}C \tag{5}$$

(An alternate derivation is given in Appendix 9.2.)

4.2 Material Balance

By assuming a film diffusion controlled model and a well-mixed suspension within the annular cell, i.e., negligible concentration gradients in the bulk fluid phase, the following steady state material balance for continuous operation can be stipulated:

$$FC_o - FC = k\overline{A}C \tag{6}$$

After rearranging and substituting the area for mean resin radius and volume, Eq. (6) becomes

$$\frac{C_o - C}{C} = \frac{3k\overline{V}}{\overline{R}\ F} \tag{7}$$

For the case where $C_o >> C$, Eq. (7) reduces to

$$\frac{C}{C_o} \cong \frac{\overline{R}\ F}{3k\overline{V}} \tag{1}$$

which relates adsorption efficiency to the primary operating variables and the overall mass transfer coefficient.

4.3 Mass Transfer Coefficient Correlations

A number of studies have been conducted to identify a general correlation for the prediction of mass transfer coefficients for suspended spheres in agitated media. The literature was reviewed (1, 3, 6, 8, 16, 25) to find a correlation for future design work.

4.3.1 Power Per Unit Volume

Brian, Hales, and Sherwood (3) have postulated that the Sherwood number for mass transfer in a stirred tank (isotropic turbulence) is a function of several dimensionless groups including a power per unit volume group, the Schmidt number, a gravity, and a density group:

$$N_{Sh} = f\left[\frac{\frac{P}{V}\, d^4 \rho_L^2}{\mu_L^3},\ N_{Sc},\ \frac{g d^3 (\rho_S - \rho_L)\rho_L}{\mu^2},\ \frac{\rho_S}{\rho_L}\right] \tag{8}$$

where:

N_{Sh} = Sherwood number, $kd/\mathcal{D}$

d = particle diameter

P = power

μ_L = fluid viscosity

ρ_L, ρ_S = density of fluid and solid

N_{Sc} = Schmidt number, $\mu/\rho_L\mathcal{D}$

The basis for the power per unit volume group is the Kolmogoroff theory of isotropic turbulence (3, 15) which depicts the transfer of kinetic energy from the mechanical agitation to the general flow of the system through a series of progressively smaller eddies until it is finally dissipated. These microscopic eddies are considered isotropic since they contain no orientation or memory of the mechanical energy input and as such represent the primary contribution to fluid turbulence.

Calculation of the power input to this particular fluid system (see Appendix 9.1.5) is theoretically possible using the friction factor data compiled for cylinders rotating in annular spaces (2, 5, 21, 23, 26). Since the primary fluid and particle motion was induced by the rotor in this study, the gravity and density groups were not considered important (density difference less than 0.1 g/cc and particle diameters less than 210 μ).

4.3.2 Slip Velocity Concept

Harriott (8) has suggested that the Sherwood number will vary from the limiting case of transfer to a sphere in a stagnant media ($N_{Sh} = 2$) with the Reynolds number and Schmidt number.

$$N_{Sh} - 2 = f(N_{Re}, N_{Sc}) \tag{9}$$

where the Reynolds number is based on the slip velocity which is defined by the relative motion of the fluid past the particle. A minimum value of the mass transfer coefficient for suspended solids is reached when the slip velocity is equal to the particle's terminal velocity. However, estimation of the actual slip velocity in a turbulent flow field, and therefore the increase over the minimum coefficient, is a complex problem to which no fully adequate solution is available.

5. RESULTS AND DISCUSSION OF RESULTS

5.1 Effect of Flow Rate

Based on material balance considerations [Eq. (7)] the relative effluent concentration, C/C_o, should vary proportionately with flow rate for a constant mass transfer coefficient. The assumptions detailed in Sect. 4.2 are verified by the results illustrated in Fig. 3. Adsorption decreases with increasing flow rate. The evident dependency on solution concentration is strong evidence supporting the initial assumption of film-diffusion being the controlling step. The flow rate range of 125 to 1500 ml/min corresponds to mean residence times from 3.0 to 0.2 min, respectively. Maximum deviation from the estimated curves is approximately 15% (see Appendix 9.6 for details). Little variation in adsorption is noted for low level changes in resin content (6 - 0.7% volume fraction).

The demonstrated linearity and unity slope of each curve suggest a constant mass transfer coefficient, k, over the extent of experimental flow rates. The contribution of axial flow (feed) to the total fluid motion or mass transfer coefficient is insignificant. (N_{Re} for the rotating motion are approximately 1000 times greater than the axial N_{Re}.) As the axial flow reaches a magnitude comparable to total fluid motion, a strong effect on mass transfer resistance would be expected. Selke and Bliss (22) report transfer coefficients vary with liquid velocity to the 0.7 power in fixed beds (axial flow constitutes the only hydrodynamic motion).

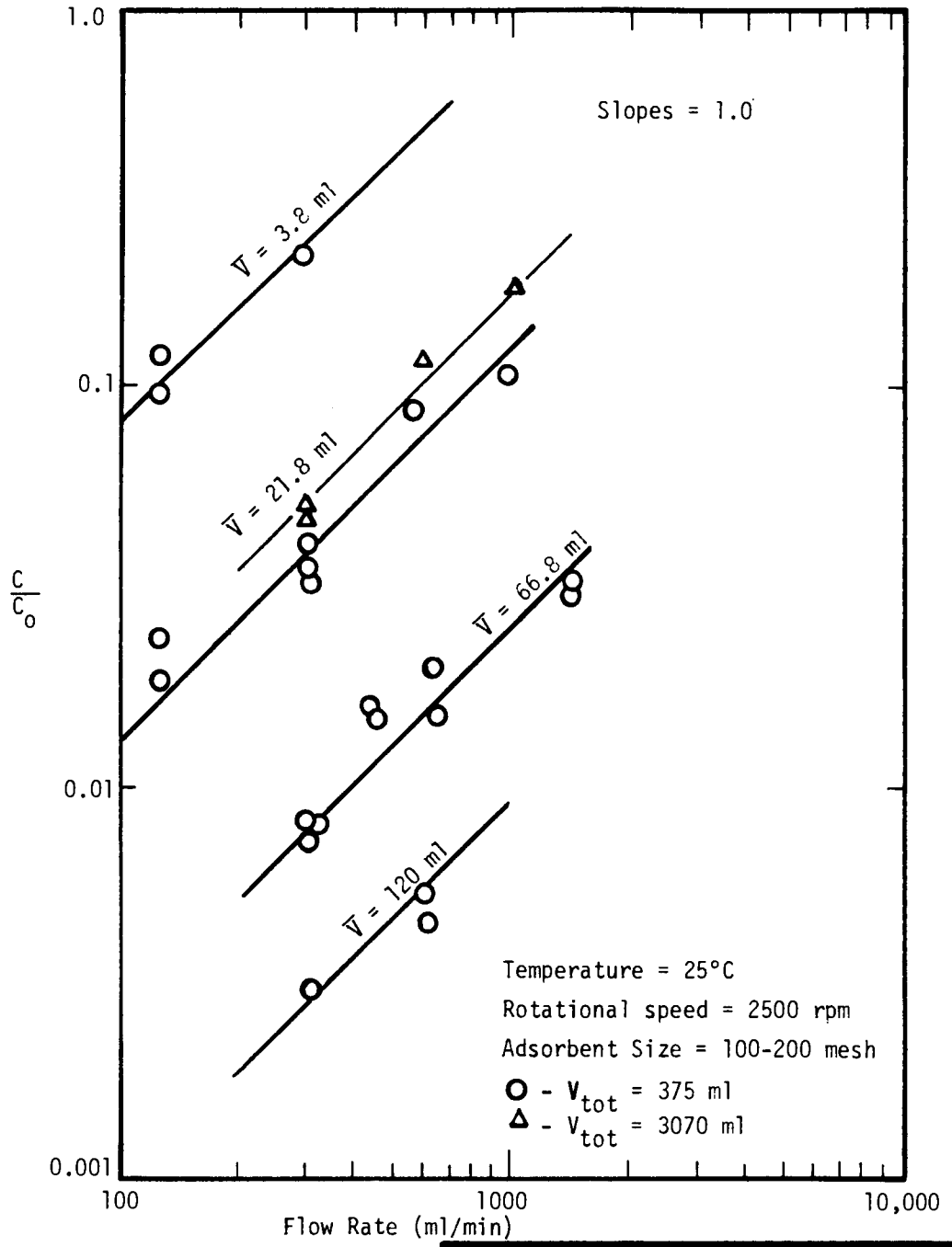

MASSACHUSETTS INSTITUTE OF TECHNOLOGY
SCHOOL OF CHEMICAL ENGINEERING PRACTICE
AT
OAK RIDGE NATIONAL LABORATORY

EFFECT OF FLOW RATE ON
Cu(II) ADSORPTION

DATE	DRAWN BY	FILE NO.	FIG.
4-22-71	DBA	CEPS-X-129	3

5.2 Effect of Resin Volume

The effect of the volume of ion exchange resin is most significant in terms of the surface area it provides for mass transfer. Figure 4 demonstrates the experimental relationship of the derived concentration parameter, $(C_0-C)/C$, to the resin volume present. As expected, it increases with unity slope until the resin volume reaches 67 ml (18% volume fraction), after which the adsorption efficiency increases disproportionately indicating an improved mass transfer coefficient. With the available equipment (1/5 hp motor and a 20 psig feed line) operation with 50 to 60% solids (approaching the value for a packed bed) was impossible.

Figure 5 characterizes the behavior of the mass transfer coefficient with respect to the volume fraction of solids. While the coefficient is obviously improved at high solids concentrations, the increased scatter in experimental data offers little evidence of the mechanism. A very simplified view, in terms of the film diffusion model, might conceptually be increased particle interactions which wipe away portions of the film, thereby increasing the value of k for a given diffusivity.

Hales (6) presents a derivation for the Sherwood number as a function of particle concentration in a stagnant medium. (Pertinent equations are given in Appendix 9.3.) As a first approximation the percentage increase in the mass transfer coefficient predicted from this formulation has been plotted in Fig. 5. This correlation tends to over estimate the influence of the solids concentration even though the derivation does not account for the relative motion between fluid and particle.

Most of the experimental work reviewed in the literature involved very low solids inventories. Harriott (8) varied the solids fraction from 0.1 to 5.5 volume percent and observed no effect on the mass transfer coefficient. He claimed this would be valid to 15% solids content, but beyond that an increasing coefficient should be expected, especially with small particles. Sykes and Gomezplata (25) found no change in the value of k with solid fractions ranging from 3 to 10%. Barker and Treybal (1) experimented with particle concentrations as high as 23% and reported a trend of larger coefficients as the solids fraction increased. As a consequence of the minimal experimental evidence, little theory has been developed to explain the phenomenon.

5.3 Effect of Resin Diameter

Figure 6 shows that as particle diameter increases, the mass transfer coefficient is reduced. Direct interpretation of the plot would imply that k is proportional to $d^{-0.5}$. However, only a relatively narrow range of particle diameters were considered (80 to 300 μ), and there was a rather large particle size distribution within any given sample (see Appendix 9.1.7).

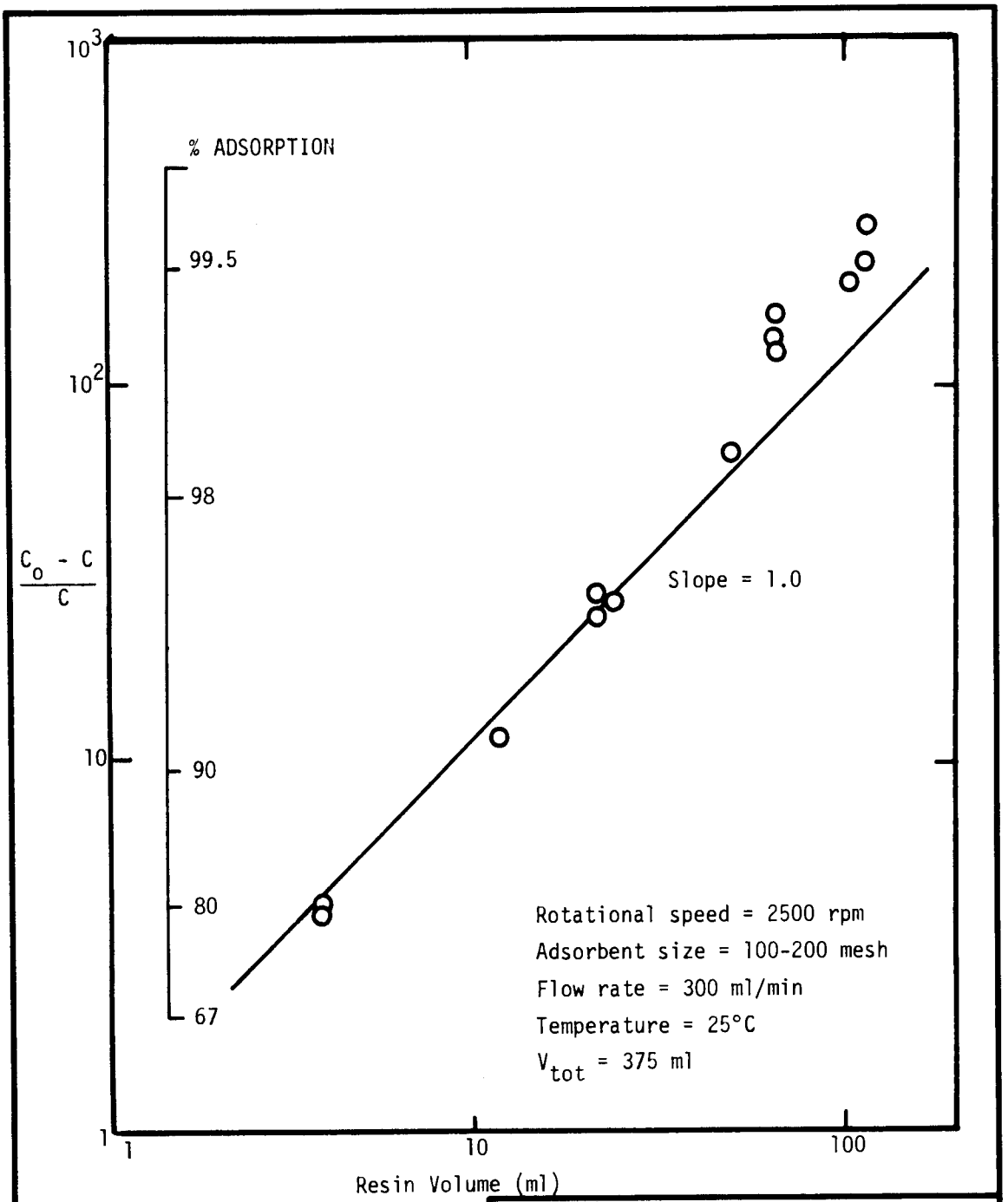

MASSACHUSETTS INSTITUTE OF TECHNOLOGY
SCHOOL OF CHEMICAL ENGINEERING PRACTICE
AT
OAK RIDGE NATIONAL LABORATORY

EFFECT OF RESIN VOLUME ON
Cu(II) ADSORPTION

DATE	DRAWN BY	FILE NO.	FIG.
4-22-71	DBA	CEPS-X-129	4

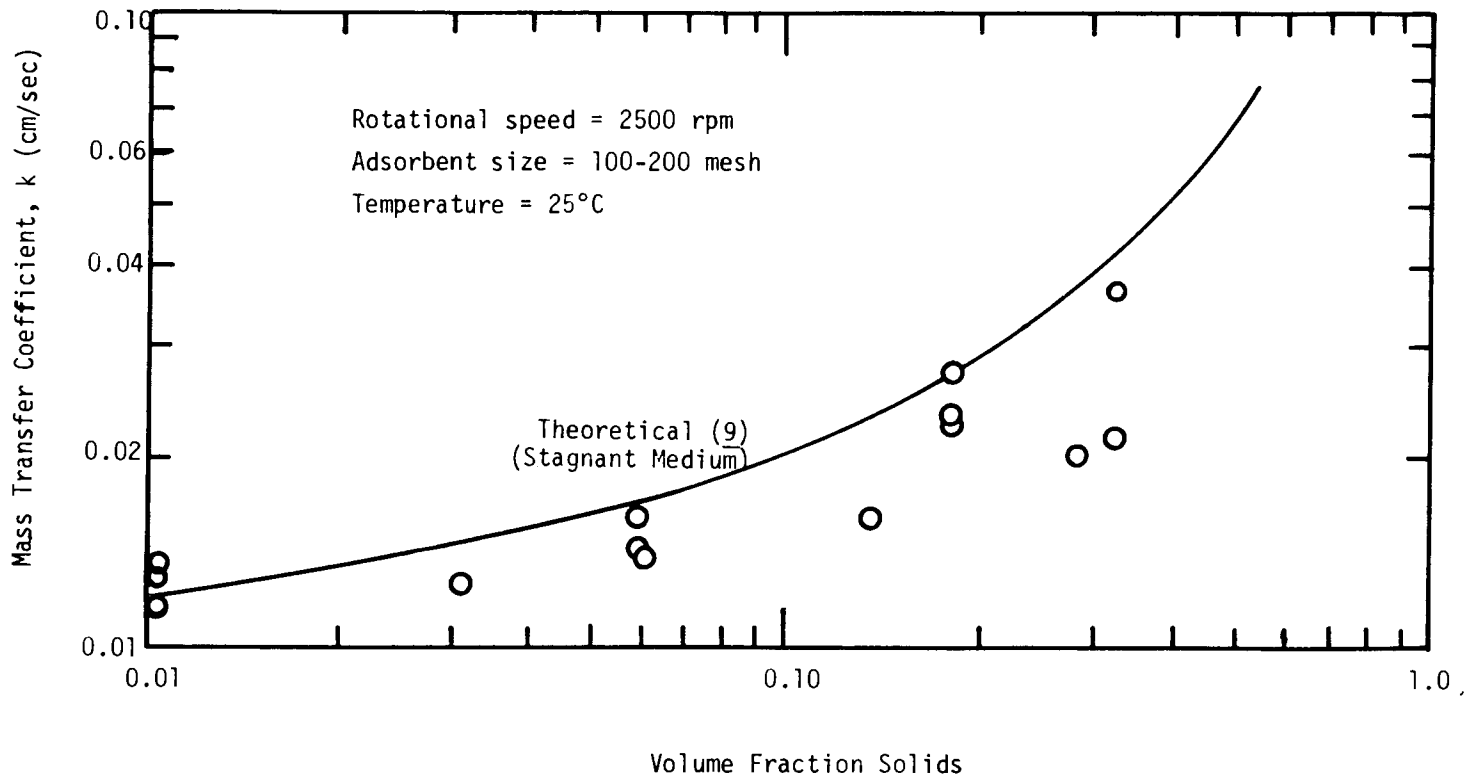

MASSACHUSETTS INSTITUTE OF TECHNOLOGY
SCHOOL OF CHEMICAL ENGINEERING PRACTICE
AT
OAK RIDGE NATIONAL LABORATORY

EFFECT OF SOLIDS FRACTION ON
MASS TRANSFER COEFFICIENT

DATE	DRAWN BY	FILE NO.	FIG.
4-25-71	DBA	CEPS-X-129	5

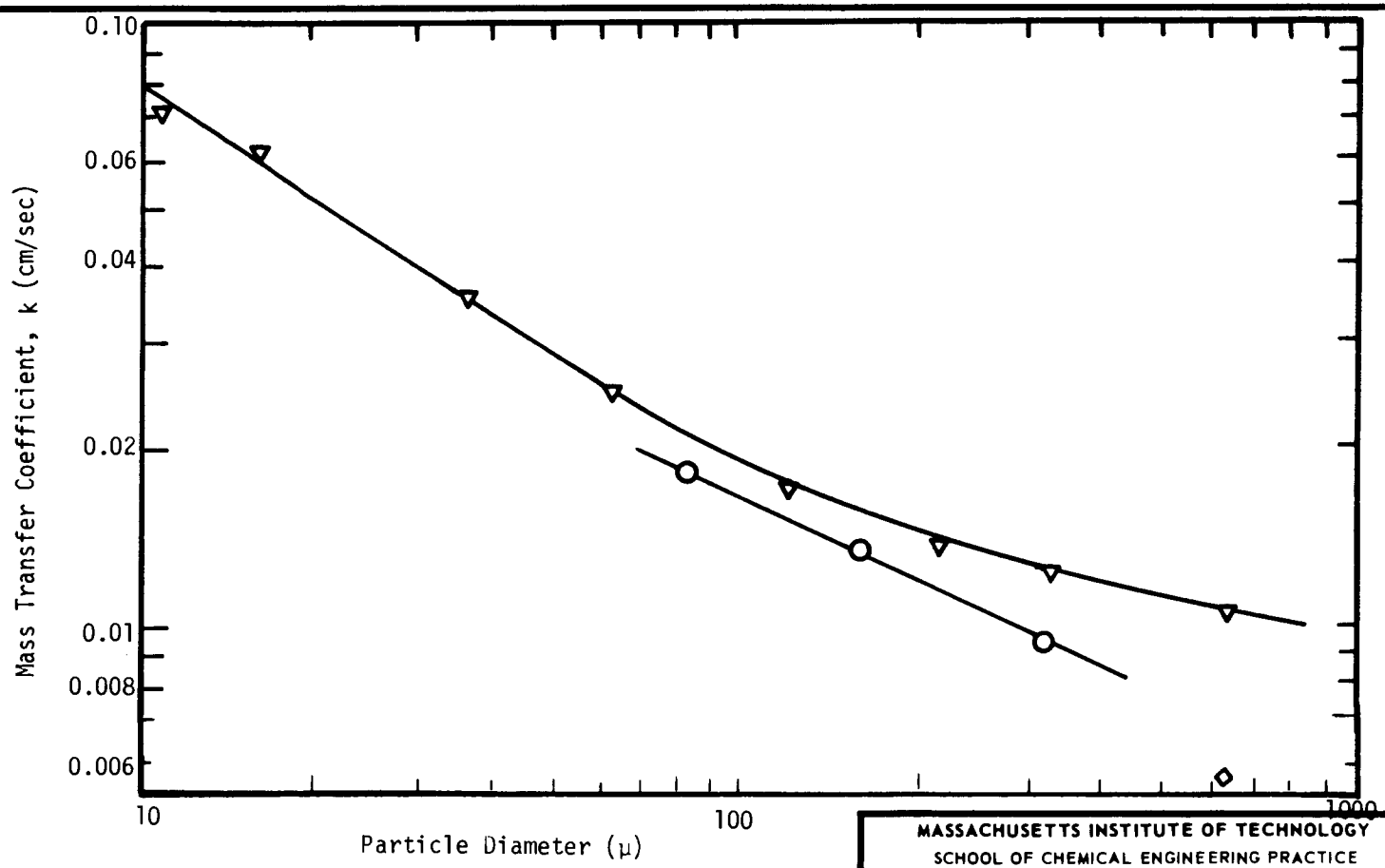

	Investigator	Ions Used	Temp. (°C)	Agitation	Apparatus
▽ -	Harriot (8)	Na^+	20	300 rpm	Tank
○ -	This Study	Cu^{++}	25	2500 rpm	Axial Filtration
◇ -	Selke-Bliss (22)	Cu^{++}	20	-	Fixed Bed

MASSACHUSETTS INSTITUTE OF TECHNOLOGY
SCHOOL OF CHEMICAL ENGINEERING PRACTICE
AT
OAK RIDGE NATIONAL LABORATORY

EFFECT OF PARTICLE SIZE ON MASS TRANSFER

DATE	DRAWN BY	FILE NO.	FIG.
4-22-71	PHW	CEPS-X-129	6

Nevertheless there is remarkable agreement between the results of this study and the data reported by Harriott (8), a portion of which has been included in Fig. 6. Harriott studied particle diameters ranging from 10 to 1000 μ for volume fractions less than 5% and found the relationship for k to vary from inverse proportionality (limiting case for small particles where $N_{Sh} = 2$) to independency of particle diameter (for very large beads). Selke and Bliss (22) report lower coefficients at larger diameters (k = 0.0055 cm/sec for $\bar{d}$ = 600 μ) from their fixed bed experiments.

5.4 Effect of Temperature

Two experimental runs were conducted at elevated temperatures (40 and 55°C). The dramatic increase in the mass transfer coefficient is illustrated in Fig. 7, where the coefficient is plotted versus the reciprocal absolute temperature. Similar increases were observed by Harriott (8) and Selke and Bliss (22). A general rule-of-thumb for rate increases due to small temperature changes is about 3-5%/°C for film diffusion and 4-8%/°C for particle diffusion (9). The experimental data from this study indicates a 4.5% increase per °C. The work of Selke and Bliss gives a similar figure while Harriott's data imply 3.3%/°C.

These results can be examined in terms of an activation energy for the diffusional process. If an Arrhenius model is postulated,

$$k \;\alpha\; e^{-E_A/RT} \tag{10}$$

the mass transfer coefficient can be related to the reciprocal of the absolute temperature, and an activation energy may be obtained from the slope. The value determined was about 6 kcal/mole which compares favorably to the data of Selke and Bliss. Harriott's results give a figure of 4.2 kcal/mole.

The activation energy concept can also help identify the process mechanisms. Liquid phase diffusion typically has an activation energy of 3-6 kcal/mole while that for internal particle diffusion varies from 6-10 kcal/mole (9). Chemical reactions generally involve levels considerably higher.

5.5 Effect of Rotational Speed and Annular Gap Width

From the simplified model of a thin film surrounding each suspended sphere, the only manner in which rotational speed and the annular gap should influence mass transfer is in the induced hydrodynamic flow field seen by the particle. To analyze this phenomenon on a consistent basis, two recent correlations for transport in an agitated vessel have been examined.

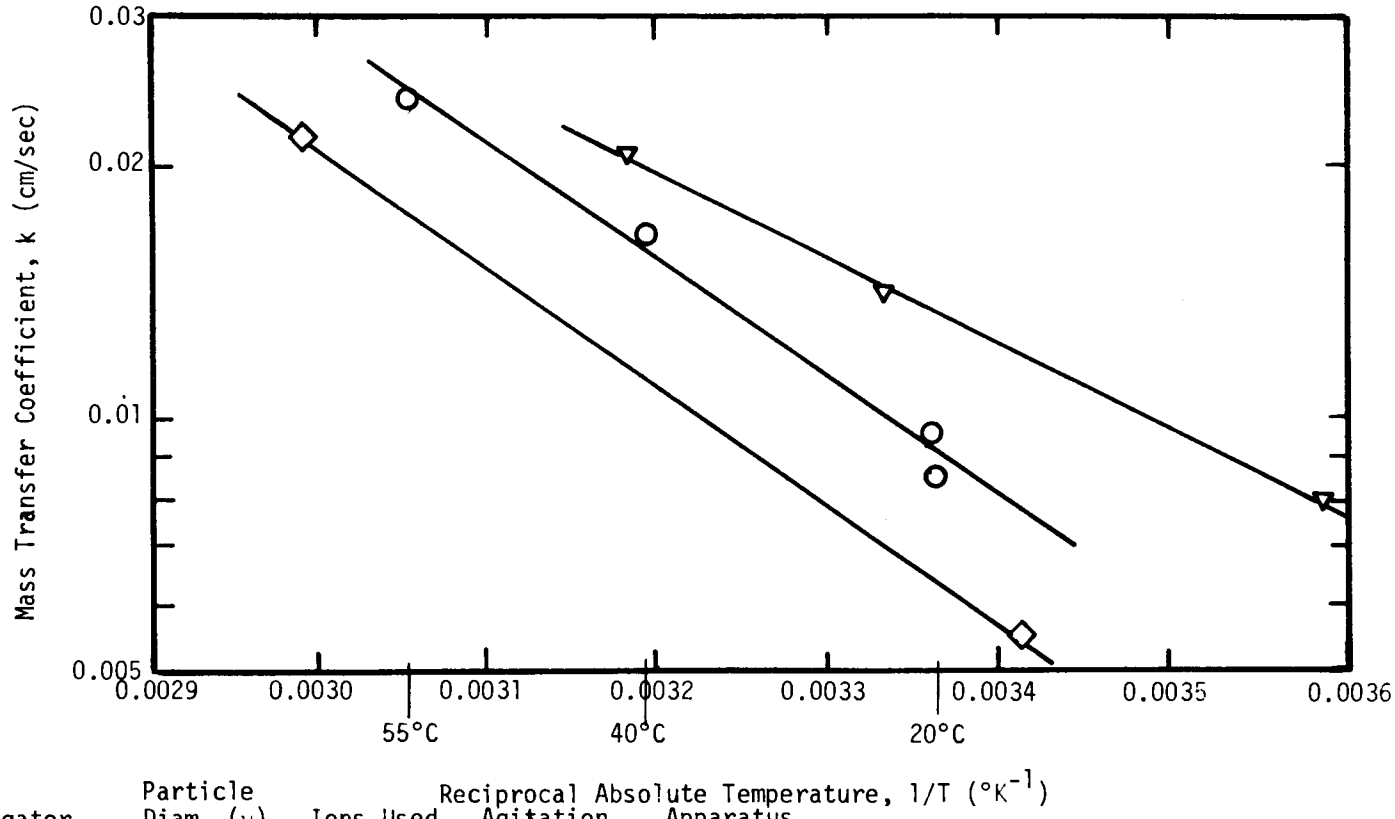

Investigator	Particle Diam. (μ)	Ions Used	Agitation	Apparatus
○ - This Study	154	Cu^{++}	300 rpm	Axial Filtration
▽ - Harriott (8)	304	Na^{+}	2500 rpm	Agitated Tank
◇ - Selke-Bliss (22)	600	Cu^{++}	-	Fixed Bed

MASSACHUSETTS INSTITUTE OF TECHNOLOGY
SCHOOL OF CHEMICAL ENGINEERING PRACTICE
AT
OAK RIDGE NATIONAL LABORATORY

ACTIVATION ENERGIES FOR DIFFUSIONAL PROCESS

DATE	DRAWN BY	FILE NO.	FIG.
9-1-71	PHW	CEPS-X-127	7

5.5.1 Power Per Unit Volume Correlation

Use of the power per unit fluid volume parameter theoretically permits correlation of mass transfer data from systems with widely varying fluid motions and geometries (3). The primary difficulty is in evaluation of the energy dissipation for a given system. With respect to a rotating cylinder in an annular space, the work of Taylor (26) provided fundamental friction factor data for estimation of inner wall shear. Sherwood and Ryan (23) have compiled the results of similar studies ($0.0279 < b/r_i < \infty$). Use of their correlations permitted calculation of the power required to maintain a designated rotational speed. (Specifics are contained in Appendix 9.1.5.) To account for the solids in the system, the suspension viscosity (14, 27) was used in the power calculations. The results are presented in Fig. 8. Calculated levels of power per unit volume range from 1.2 to 411 x 10^6 ergs/sec corresponding to abscissa values of 3 to 44. To support the confidence level of the calculated power consumption, the net energy dissipation of the fluid was experimentally measured for the large annulus (see Appendix 9.4). Good agreement was found as evidenced in Fig. 8. The difficulty of experimental determination is in the magnitude of internal frictional losses in both the motor and seals, roughly 100 times that transferred to the fluid in the case of the large annulus. For the smaller annuli, this ratio increased to an extent which prevented accurate measurement. From a practical standpoint, these losses represent a sizeable energy cost to obtain a well-mixed system. The primary variables of annular gap width and rotational speed seem well represented by this correlation. An empirical curve suggested by Hales (6) is included for comparison.

Significant discrepancies occur at high resin volumes (28%) where the calculated power per unit volume no longer characterizes the mass transfer coefficient. Several reasons are offered for this deviation, none of which are totally satisfactory. The bulk of the friction factor data describing this form of Couette flow has been based on homogeneous fluid systems without flow of fluid through the rotor. Suspension viscosity correlations (14, 27) in light of the conclusions reached by Gandhi and Estrin (5) were used to approximate the solids contribution. Unusual flow patterns were observed at high particle concentrations; in particular, accumulation of solids was seen as a formation of narrow bands encircling the annulus. Such flow phenomena are apparently not uncommon (4, 7, 11). Finally a high solids concentration can effect considerable change in the mass transfer coefficient as noted earlier. Particle interactions for these concentrations are not well understood, and subsequently, available correlations are shown to be inadequate.

5.5.2 Slip Velocity Correlation

Harriott's slip velocity correlation (8) was considered; in the simplest case a minimum transfer coefficient is based on the terminal velocity of particle (see Sect. 4.3.2). This approximation yields a k value of 0.0036 cm/sec which is independent of rotational speed and system geometry. Contrast this value with the actual data shown in Fig. 8, and the shortcomings of such

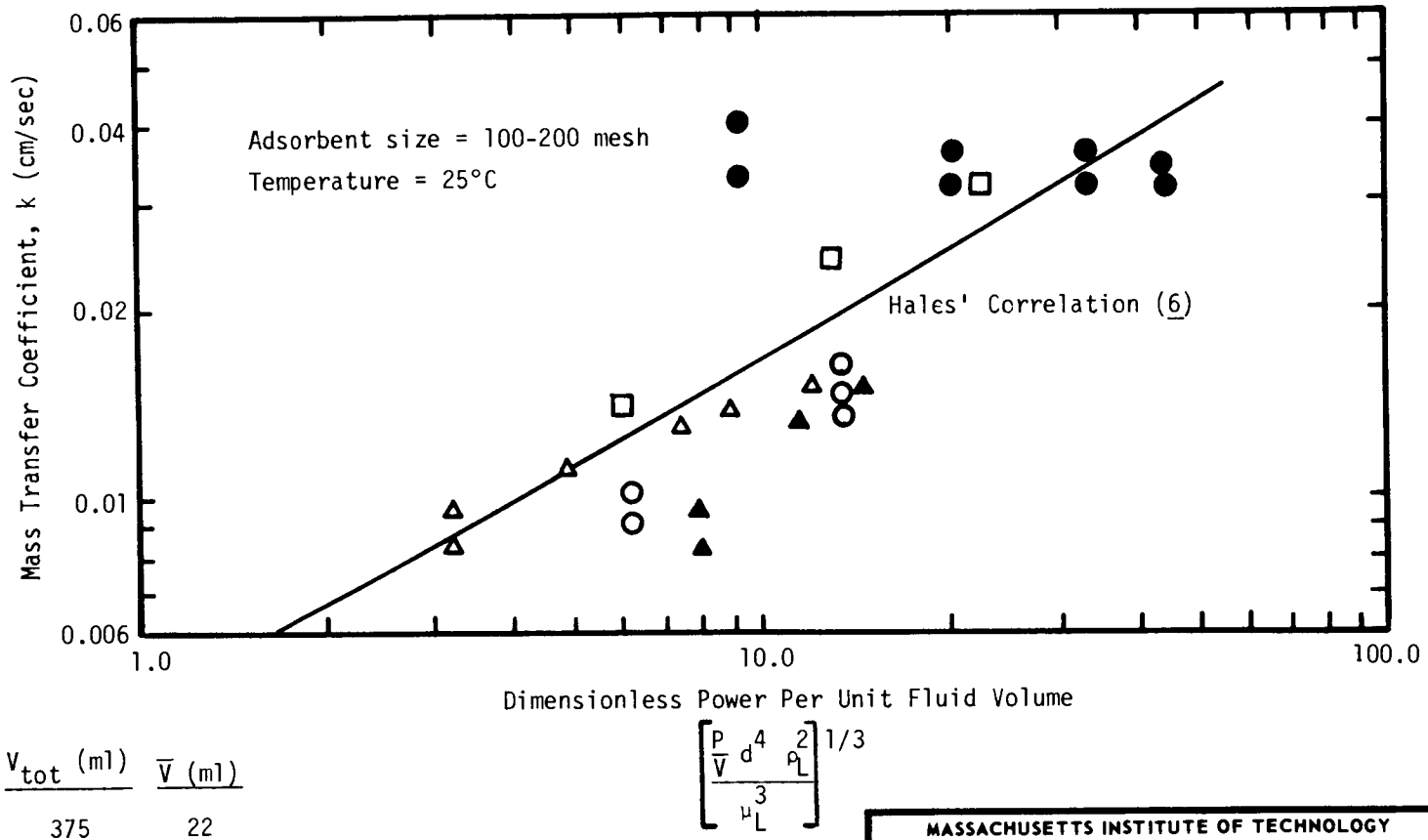

	V_{tot} (ml)	$\bar{V}$ (ml)
○ -	375	22
● -	375	104
□ -	185	22
△ -	3070	22
▲ -	3070	22*

*Power Measured Experimentally

MASSACHUSETTS INSTITUTE OF TECHNOLOGY
SCHOOL OF CHEMICAL ENGINEERING PRACTICE
AT
OAK RIDGE NATIONAL LABORATORY

CORRELATION OF MASS TRANSFER COEFFICIENTS

DATE	DRAWN BY	FILE NO.	FIG.
4-25-71	DBA	CEPS-X-129	8

a correlation are immediately apparent. Further application requires knowledge of the true slip velocity as a function of the geometry, agitation, and particle size. Unfortunately, no such correlation is available, although Harriott acknowledges that the parameter of power per unit volume correlates his data reasonably well.

5.6 Use of Generalized Correlation

All data accumulated during this investigation (except those runs with solids content higher than 20%) have been plotted in Fig. 9 ($N_{Sc} \sim 1000$). Harriott's data for ion exchange with sodium ($N_{Sc} \sim 500$) and Hałes' correlation have been included for comparison. The data are reasonably well predicted (mean deviation 15.4%) in the region of investigation by the expression

$$N_{Sh} = 0.87 \left[\frac{\frac{P}{V} d^4 \rho_L^2}{\mu_L^3} \right]^{n/3} N_{Sc}^{1/3} \qquad (2)$$

where the constants 0.87 and n = 0.4 were determined from the figure.

The correlation agrees fairly well with the individual findings of the project; even so, some caution should be exercised in extrapolating the results. Equation (2) predicts that k varies with particle diameter to the -0.47 power compared with the -0.5 power discussed earlier. The temperature dependence of k in the equation is derived in Appendix 9.5, and the activation energy is 4 kcal/mole compared with the experimental value of 6 kcal/mole. The primary weakness of this correlation is that it cannot accommodate high resin volumes.

5.7 Large-Scale Implications

The secondary objective of this study was to offer a basis for large-scale design. In addition to the correlations reviewed, several economic or performance factors were also considered (product flux, pressure drop, adsorption efficiency, and design alterations). Table 1 gives several examples of experimental product flux achieved which range from 1000 to 15,000 gpd/ft^2 for pressure drops less than 4 psi and adsorption efficiencies as high as 99+%.

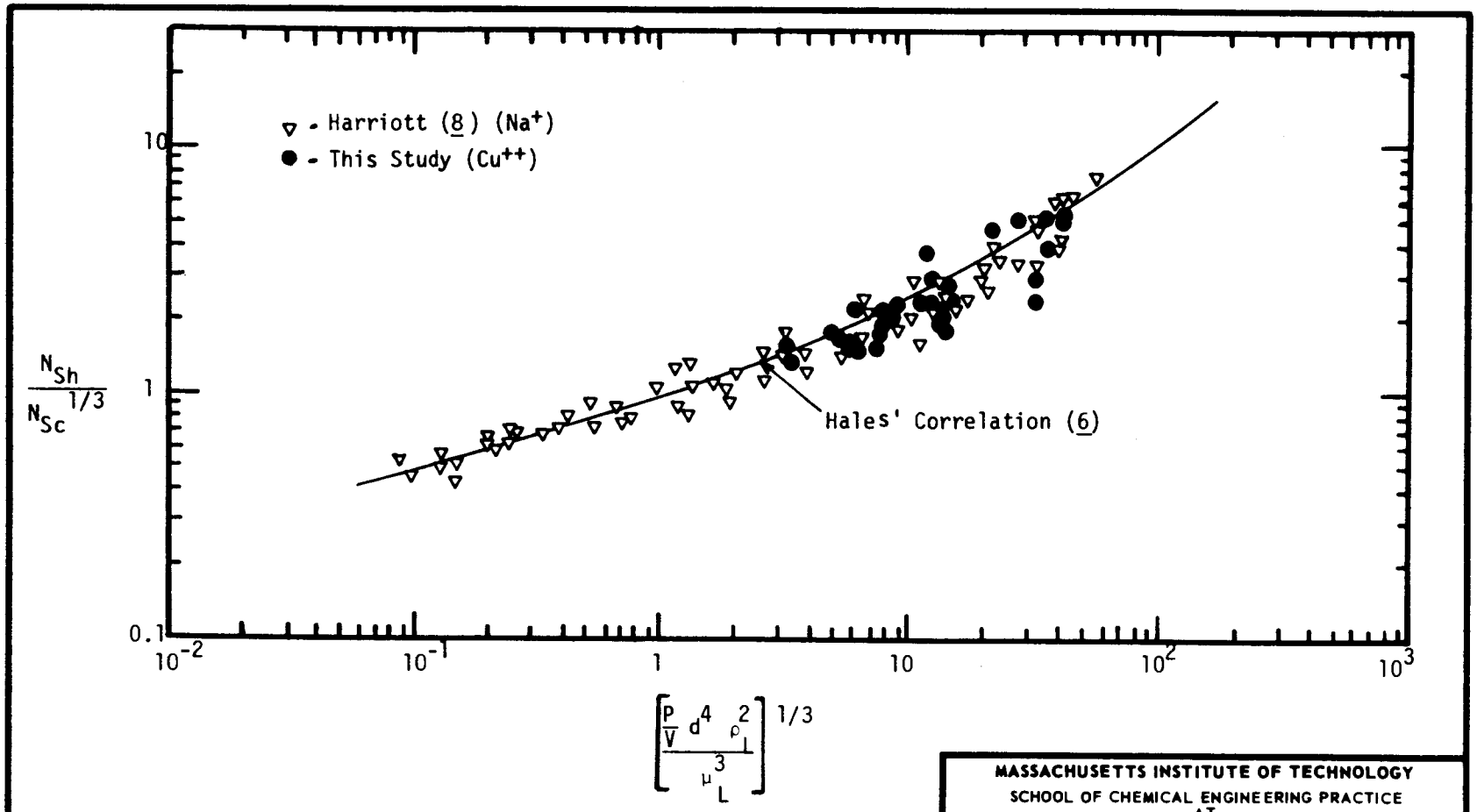

Data for $\overline{V}/V_{tot} < 0.20$

MASSACHUSETTS INSTITUTE OF TECHNOLOGY
SCHOOL OF CHEMICAL ENGINEERING PRACTICE
AT
OAK RIDGE NATIONAL LABORATORY

GENERAL CORRELATION FOR TRANSPORT DATA

DATE	DRAWN BY	FILE NO.	FIG.
4-27-71	DBA	CEPS-X-129	9

Table 1. Performance Factors at 25°C and 2500 rpm

Sample	Flux (gpd/ft2)	Efficiency (%)	ΔP (psi)	$\overline{V}/V_T$
67-4A	1300	98.1	1	0.058
76-5	3000	99.7	1	0.320
77-6	6000	99.5	1.5	0.320
91-3A	15,200	96.9	4.0	0.176

(Experimental details are included in Appendix 9.7.)

One unique advantage of this system is the use of the centrifugal force field to shield the filter surface from residue accumulation. Operation with large fluid volumes, however, will necessitate more efficient transfer of energy to the fluid. To accomplish this, and at the same time avoid extremely high rotational velocities, paddles might be attached to the rotor and baffles installed in the annular gap.

An efficient means of regenerating the ion exchange resin is of industrial concern. Selke and Bliss (22) provide equations for estimation of resin exhaustion in the specific case of copper exchange.

6. CONCLUSIONS

1. Tracer copper contaminants can be removed by adsorption and filtration. High product flux (1000 - 15,000 gpd/ft^2) and adsorption efficiencies (90 - 99+%) coupled with low pressure drops (0 - 10 psi) make the system attractive for large-scale operations.

2. The general material balance coupled with a first order mass transfer expression describes the system effectively.

3. The correlation proposed by Brian, Hales, and Sherwood (3) provides a reasonable means for prediction of the mass transfer coefficient.

4. Specific findings for the mass transfer coefficient were:

   a) Independent of flow rate

   b) Increases with high resin volumes

   c) Increases with decreasing particle size

d) Increases with increasing temperature

e) Correlates well with annular gap size and rotational speed based on power per unit fluid volume.

7. RECOMMENDATIONS

1. Performance of the system at a high solids concentration should be further studied.

2. Effective elution techniques should be developed for possible industrial regeneration applications.

3. Modifications of the unit (agitation paddles and baffles) should be considered to improve the mixing efficiency and application potential of the system.

8. ACKNOWLEDGEMENTS

The authors wish to thank their consultant, Fred Nelson, for his valuable help in the theoretical and experimental development of this study. In addition, thanks are also given to K.A. Kraus, L. Dresner, and D.G. Thomas for their helpful comments.

9. APPENDIX

9.1 Sample Calculations

9.1.1 Ion Exchange Resin Capacity

The cation exchange resin (hydrogen form), Dowex 50W-X12, was employed throughout the investigation. Capacity specifications were given as 2.3 meq/ml of resin bed (9). Based on the suggestion by Nelson (17), a void volume of 40% was assumed for the wet resin bed.

For 36.8 ml of wet resin bed (22 ml of actual resin):

$$\text{total } Cu^{++} \text{ adsorption capacity} = \left(\frac{2.3 \text{ meq}}{\text{ml resin bed}}\right)\left(\frac{1 \text{ mmole } Cu^{++}}{2 \text{ meq}}\right) \times (36.8 \text{ ml resin bed})$$

$$= 42.4 \text{ mmoles } Cu^{++}$$

Since the inlet feed concentration was approximately 4×10^{-6} M Cu^{++},

$$\frac{42.4 \text{ mmoles } Cu^{++}}{4 \times 10^{-6} \text{ M } Cu^{++}} = 10.6 \times 10^{6} \text{ ml } Cu^{++} \text{ allowable throughput}$$

Under experimental conditions, the resin was never loaded to more than 5% capacity.

9.1.2 Activity of Tracer

If a 10 mg sample of $Cu(NO_3)_2 \cdot 3H_2O$ were irradiated for 10 min, the activity (in disintegrations/sec) can be calculated from

$$A' = N F_0 \sigma S \qquad (11)$$

where:

A' = activity, dis/sec

N = number of atoms of target nuclide

F_0 = neutrons/cm^2/sec, about 10^{14}

σ = activation cross section for reaction, 4.5 barns (4.5×10^{-24} cm^2/atom)

S = saturation factor, ratio of activity produced in time t to that produced in infinite time

$= 1 - e^{\lambda t}$

λ = 0.693/half life

$$N = \left(\frac{0.010 \text{ gm sample}}{241.6 \text{ g/gmole}}\right)(6.02 \times 10^{23} \text{ atoms/gmole})\left(\frac{0.69\ {}^{63}Cu}{Cu_{total}}\right)$$

$$= 17.2 \times 10^{18} \text{ atoms } {}^{63}Cu$$

Since the half life of ^{64}Cu is 12.8 hr,

$$S = 1 - e^{-0.693(10)/(60)(12.8)} = 0.0089$$

Therefore,

$$A' = (17.2)(10^{18})(10^{14})(4.5)(10^{-24})(0.0089)$$

$$= 0.695 \times 10^{8} \text{ dis/sec} = 6.95 \times 10^{7} \text{ dis/sec}$$

Note: Since 31% of the naturally occurring copper is ^{65}Cu (σ = 1.9 barns), a portion of the irradiated sample will contain ^{66}Cu (half life = 5.1 min); however, no tracer was introduced into the system within one hour of irradiation.

9.1.3 Evaluation of Experimental Data

Example: Run 67-5A taken from Databook A-5508-G, pp. 67 and 73.

Run conditions:

flow rate = ∿300 ml/min

resin volume = 21.84 cc (36.4 cc resin bed)

resin size = 100 - 200 mesh (70 - 170 wet basis)

annular volume = 375 ml

rotational speed = 2500 rpm

temperature = 25 - 27°C

Databook entries:

effluent sample collection = 483 ml/1.60 min

average flow rate of contaminated solution = 2.28 ml/min

pressure drop for filter $\approx$ 1 psi

radiometric analysis:

average background = 4340 counts/800 sec

2.0 ml contaminated solution (average based on t = 0) = 40,884 counts/80 sec

sample 5A concentrated = 29,942 counts/800 sec (t = 170 min)

amount of contaminated solution in effluent sample = 2.38 ml/min x (1.60 min) = 3.65 ml

Net activity of standard charge solution:

$$\frac{40{,}884 \text{ counts/80 sec} - 434 \text{ background counts/80 sec}}{2 \text{ ml}} = 20{,}225 \text{ counts/80 sec-ml}$$

Net activity sample per ml:

$$\frac{2994 \text{ counts/80 sec} - 434 \text{ bkgd counts/80 sec}}{3.65 \text{ ml}}(1.17) = 821 \text{ counts/80 sec-ml}$$

where 1.17 is the time factor allowance for ^{64}Cu decay during the 170 min time lapse. This factor may be calculated from the expression:

$$F^* = e^{0.693t/t_{1/2}}$$

Adsorption ratio,

$$C/C_o = 821/20{,}225 = 0.041$$

Concentration parameter,

$$(C_o - C)/C = (1/0.041) - 1 = 23.4$$

Mass transfer coefficient,

$$k = \left(\frac{C_o - C}{C}\right) \frac{F\bar{R}}{3\bar{V}} = \frac{(23.4)(300\ \text{ml/min})(0.0077\ \text{cm})}{(3)(60\ \text{sec/min})(21.84\ \text{ml})} = 0.0138\ \text{cm/sec}$$

9.1.4 Equilibrium Distribution of Copper (II)

In the presence of an electrolyte the process of ion exchange can be represented as an equilibrium reaction,

$$2RH + Cu^{++} \rightleftharpoons R_2Cu + 2H^+ \tag{12}$$

where R is the sulfonic acid group of the resin. The equilibrium expression for this equation (assuming unity activity coefficients) is

$$k_c = \frac{[Cu]_R}{[Cu^{++}]} \cdot \frac{[H^+]^2}{[H]_R^2} \tag{13}$$

The distribution coefficient, D_v is defined as the concentration ratio of copper in the resin to that in solution.

$$D_v = \frac{[Cu]_R}{[Cu^{++}]} \tag{14}$$

Under conditions where only a small portion of resin capacity is used, the concentration of hydrogen in the resin is effectively unchanged, thereby giving

$$\frac{d \log D_v}{d \log [H^+]} = -2 \tag{15}$$

Reported data (24) for the distribution coefficient of copper (II) in a nitric acid media is graphically illustrated in Fig. 10. The data were obtained with Dowex 50-X8 at 40% loading (this study ∿5%). An experimental slope of -1.62 was considered conservative for an extrapolation to the conditions of this study. Example: For a solution of 10^{-3} M HNO_3 the estimated distribution coefficient is approximately 10^6. In other words, at equilibrium the ratio of copper (II) per ml of resin to copper (II) per ml of solution is one million to one.

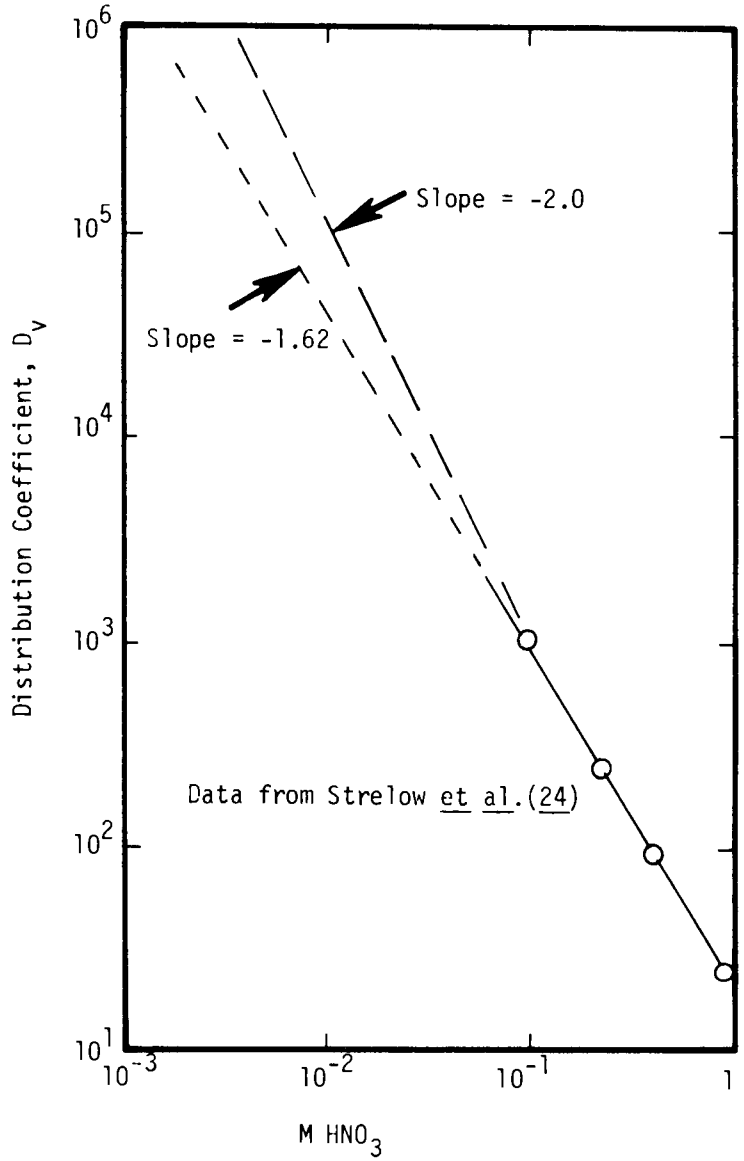

MASSACHUSETTS INSTITUTE OF TECHNOLOGY
SCHOOL OF CHEMICAL ENGINEERING PRACTICE
AT
OAK RIDGE NATIONAL LABORATORY

EQUILIBRIUM DISTRIBUTION COEFFICIENT
[Cu(II) in HNO_3]

DATE	DRAWN BY	FILE NO.	FIG.
4-25-71	PHW	CEPS-X-129	10

9.1.5 Power Per Unit Volume

Example: Run 67-5A

System dimensions:

rotor radius = 1.65 cm = r_i

cylinder radius = 3.17 cm = r_o

annular gap = 1.52 cm = b

rotor length = 13.3 cm = ℓ

Using friction factor data compilation of Sherwood and Ryan (23),

$$N_{Re} = \frac{2\, r_i\, U_i\, \rho_L}{\mu_L \mu_r}$$

where the tangential velocity and relative viscosity of the suspension are introduced.

$$U_i = 2\pi r_i \left(\frac{\omega}{60}\right) = 425 \text{ cm/sec for } \omega = 2500 \text{ rpm}$$

For 6% solids,

ρ_L = 1.01 gm/cm^3

μ_L = 0.8937×10^{-2} gm/cm-sec for pure water at 25°C

μ_r = 1.1 from Lee (14)

N_{Re} = 142,500

$f \cong 0.003$ for r_o/r_i = 1.92

power = $\tau_i\, A\, U_i$

$A = 2\pi r_i \ell$ = 138 cm^3

$$\tau_i = \frac{f\, \rho_L\, U_i^2}{2} = 274 \text{ dyne/cm}^2$$

power = 15.6×10^6 erg/sec

power per unit volume of fluid = 15.6×10^6 erg/sec/(375 ml - 21.84 ml)

= 44.2 erg/sec-ml

dimensionless power per unit volume factor = $\left(\frac{P}{V}\frac{d^4 \rho_L^2}{\mu_L}\right)^{1/3} = 13.3$

9.1.6 Diffusion Coefficient

Diffusivities for dilute aqueous electrolyte solutions may be estimated from the Nernst equation (19, 20).

$$\mathcal{D} = \frac{RT}{F^2}\left[\frac{\lambda_+^\circ \lambda_-^\circ}{\lambda_+^\circ + \lambda_-^\circ}\right]\left[\frac{Z_+ + Z_-}{Z_+ Z_-}\right] \qquad (16)$$

where:

$\mathcal{D}$ = diffusion coefficient, cm^2/sec

T = absolute temperature, °K

λ_+°, λ_-° = limiting ionic conductances for cation and ion, mho/equivalent

Z_+, Z_- = ion valences for cation and anion (absolute, i.e., no sign)

F = Faraday's constant

For the case of copper-hydrogen cationic exchange, this relationship reduces to

$$\mathcal{D}_{Cu(II)} = \frac{RT\ \lambda_+^\circ}{F^2\ Z_+}$$

where:

	Cu^{++}	Na^+	OH^-
λ° mho/equivalent	54	197.6	50.1
Z	2	1	1
T (°K)	298	298	298

and

$$\mathcal{D} = 0.72 \times 10^{-5} \text{ cm}^2/\text{sec}$$

For the case of NaOH, where a neutralization reaction is occurring,

$$\mathcal{D}_{NaOH} = 8.931 \times 10^{-10}\, T\left(\frac{197.6(50.1)}{247.7}\right)\left(\frac{2}{1}\right) = 2.13 \times 10^{-5} \text{ cm}^2/\text{sec}$$

Values for limiting ionic conductances were taken from Reid and Sherwood (19).

9.1.7 Mean Particle Size

For a Dowex 50W-X12 resin of 100-200 dry mesh size, the wet mesh size (swollen state) is 70 - 170. From tables of the U.S. Standard Screen Series (9), wet mesh size corresponds to radii from 0.011 to 0.0044 cm. An arithmetic average over the range gives the mean wet particle diameter as 154 μ. An experimental particle size distribution was obtained for 109 wet particles. Since the most significant geometrical contribution to the hydrodynamic boundary layer and mass transfer is the area of the sphere, an area-average mean diameter was calculated.

$$\bar{d} = \frac{\Sigma \bar{A}_i d_i}{\Sigma \bar{A}_i} = \frac{\Sigma n_i d_i^3}{\Sigma n_i d_i^2} = 146\ \mu$$

This value compares favorably with the arithmetic average of the range, 154 μ. The arithmetic averages were used in all the calculations and figures.

9.1.8 Mass Transfer Coefficient (Batch Operation)

A batch operation was run with a 1000-ml beaker and a small magnetic stirrer with the 200-400 mesh size resin to determine the mass transfer coefficient for comparison to the flow system. Using Eq. (17) from Appendix 9.2, one finds:

$$t = -\frac{R\,\delta\,V}{3\,\bar{V}\,\mathcal{D}}\,\ell n\,\frac{C}{C_o} \qquad (17)$$

$$k = \frac{\mathcal{D}}{\delta} = -\frac{RV}{3\bar{V}}\,\frac{\ell n\ C/C_o}{t} \qquad (4)$$

$$= -\frac{(0.004 \text{ cm})(1000 \text{ ml})}{3(0.9 \text{ ml})(10 \text{ min})(60 \text{ sec/min})}\,\ell n\,\frac{2866}{28{,}806} = 0.0056 \text{ cm/sec}$$

9.1.9 Dimensionless Groups

Sherwood number (mass transfer Nusselt number), $N_{Sh} = \frac{kd}{\mathcal{D}}$

Schmidt number, $N_{Sc} = \frac{\mu}{\rho\mathcal{D}}$

System properties (25°C):

for a 100-200 mesh resin = 0.0154 cm (0.0146 cm, area - average mean) wet resin

ρ = 1.0 gm/cm^3

μ = 0.8937×10^{-2} gm/cm-sec

$\mathcal{D} \approx 10^{-5}$ cm^2/sec(0.72×10^{-5} cm^2/sec from Eq. 16) (a value of 10^{-5} was used in the power correlation)

k = 0.0138 cm/sec (Run 67-5A)

$$N_{Sh}/N_{Sc}^{1/3} = (kd/\mathcal{D})/(\mu/\rho\mathcal{D})^{1/3} = 2.2$$

9.2 Alternate Derivation for Mass Transfer Expression

Helfferich (9) offers the following expression for the time required in film diffusion controlled isotopic ion exchange (assuming excess resin capacity available):

$$t = -\frac{\overline{R}\,\delta\,V}{3\,\overline{V}\,\mathcal{D}}\,\ell n\,\frac{C}{C_o} \qquad (17)$$

where C and C_o are solution concentrations at t = t and t = 0, respectively. Rewriting this equation in differential form, one obtains:

$$\frac{dC}{dt} = -\frac{3\,\overline{V}\,\mathcal{D}}{\overline{R}\,V\,\delta}\,C \qquad (18)$$

For spherical particles, $3\overline{V}/\overline{R}$ may be replaced with surface area, $\overline{A}$, and the mass transfer coefficient k from Eq. (4) may be substituted in Eq. (18),

$$-V\frac{dC}{dt} = k\,\overline{A}\,C \qquad (5)$$

9.3 Theoretical Model for Particle Interactions

For zero flow conditions, $N_{Pe} = 0$, the Sherwood number is given by (6):

$$N_{Sh} = \frac{2}{1 - \overline{X}} = \frac{4(R^{*3} - \overline{R}^3)}{2\,R^{*3} + \overline{R}^3 - 3\overline{R}R^{*2}} \tag{19}$$

where:

$\overline{X}$ = dimensionless bulk concentration

$\overline{R}$ = particle radius

R^* = radius of spherical shell surrounding particle

$(\frac{\overline{R}}{R^*})^3$ = volume fraction of solids present

As $R^* \longrightarrow \infty$, $N_{Sh} \longrightarrow 2$.

By basing the fractional increase in mass transfer coefficient with solids content on the value at a particle concentration of 1%, the following are obtained:

vol % Solids	$N_{Sh}/(N_{Sh}$ at 1%)
0.8	0.97
2.7	1.19
6.4	1.49
12.5	1.93
21.6	2.60
34.3	3.72
51.2	6.00

The original computations were made by Hales (6).

9.4 Procedure for Experimental Power Measurements

Determination of fluid power dissipation involved attachment of a wattmeter (0 - 100 w scale) on the motor power source. Power readings were taken

for the rotor spinning in air at different rpm levels and for the rotor spinning in water. The difference in power consumption was attributed to viscous dissipation.

Example: The large annulus ($b/r_i = 3.71$) was used and for a rotational speed of 2500 rpm, the input power when spinning in air was 50 w. For the same conditions when filled with water, the reading was 56 w. The difference, 6 w, was assumed to have been dissipated by the fluid.

$$(6\ \text{w})\left(\frac{10^7\ \text{ergs/sec}}{\text{watt}}\right) = 6 \times 10^7\ \text{ergs/sec}$$

which compares with the calculated value of 1.6×10^7 ergs/sec.

9.5 Temperature Dependence of Generalized Correlation

The correlation of Brian, Hales, and Sherwood (3) is given as:

$$N_{Sh} \propto \left(\frac{P}{V}\frac{d^4 \rho_L^2}{\mu_L^3}\right)^{n/3} N_{Sc}^{1/3} \tag{2}$$

where $n = 0.4$ for values of $\left(\frac{P}{V}\frac{d^4\rho_L^2}{\mu_L^3}\right)^{1/3}$ ranging from 4 to 44 with $N_{Sc} \sim 1000$. Therefore,

$$\frac{k}{\mathcal{D}} \propto \left(\frac{1}{\mu_L^3}\right)^{0.4/3}\left(\frac{\mu_L}{\mathcal{D}}\right)^{1/3} \tag{20}$$

$$k \propto \mathcal{D}^{0.67}\ \mu^{-0.07} \tag{21}$$

This assumes the viscosity variations in the P/V term to be negligible. From Reid and Sherwood (19),

$$\mathcal{D} \propto \frac{T}{\mu} \tag{22}$$

so that

$$k \propto (T)^{0.67}\ (\mu)^{-0.74} \tag{23}$$

The temperature dependence of the viscosity function over limited temperature ranges is well approximated by (18).

$$\mu \ \alpha \ e^{B/T} \tag{24}$$

so that

$$k \ \alpha \ (T)^{0.67} \ e^{-0.74B/T} \tag{25}$$

The value of B for water from 0 to 47°C is 2200°K (taken from Fig. 11). Upon calculation of a pseudo mass transfer coefficient according to Eq. (25) for several temperatures, an activation energy of 4 kcal/mole is determined (see Fig. 11). The experimentally observed value for the activation energy was 6 kcal/mole.

9.6 Error Analysis

Mean percent deviation for experimental data: An average percent deviation using Eq. (2) was computed for each experimental data point (except runs when $\overline{V}/V_{tot} > 0.20$) in the following manner:

Example: Run 67-5A

$$\left(\frac{P}{V}\frac{d^4 \rho_L^2}{\mu_L^3}\right)^{1/3} = 13.3$$

$$(N_{Sh}/N_{Sc}^{1/3}) = 2.20 \text{ (experimental)}$$

$$(N_{Sh}/N_{Sc}^{1/3})_{calc} = 2.45 \text{ [from Eq. (2)]}$$

$$\% \text{ deviation} = \frac{2.45 - 2.20}{2.45}(100) = 10.2\%$$

Summing the percent deviations over all the data:

$$\text{mean percent deviation} = \frac{525.6}{34} = 15.4\%$$

Estimated limits of experimental accuracy:

flow rate	± 1 ml/min
resin volume	± 1 ml (resin bed) (void fraction of 40% was assumed)

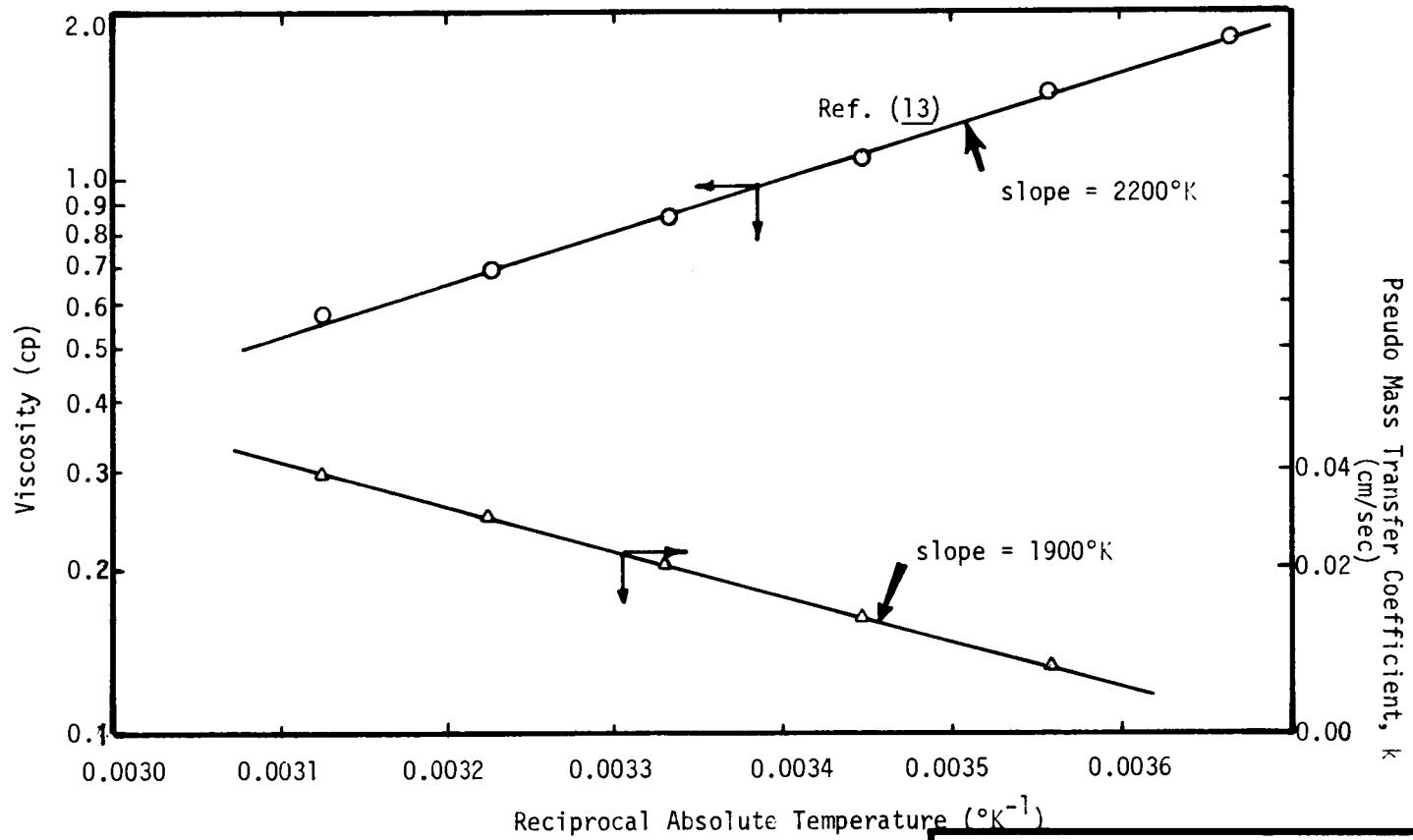

MASSACHUSETTS INSTITUTE OF TECHNOLOGY
SCHOOL OF CHEMICAL ENGINEERING PRACTICE
AT
OAK RIDGE NATIONAL LABORATORY

VISCOSITY OF WATER AS A FUNCTION OF TEMPERATURE

DATE	DRAWN BY	FILE NO.	FIG.
4-25-71	PHW	CEPS-X-127	11

particle diameter	estimated mean
temperature	$\pm$ 2°C
rotational speed	$\pm$ 25 rpm
annular gap width	$\pm$ 0.01 cm

9.7 Summary of Data and Calculated Values.

A summary of data and calculated values can be found in Table 2.

9.8 Location of Original Data

Documentation for all experimental work conducted may be found in ORNL Databook A-5508-G, pp. 54-104. Calculations and literature references are on file with the databook at the M.I.T. School of Chemical Engineering Practice, Bldg. 1000, ORNL.

9.9 Nomenclature

a	constant
A	surface area of rotor, cm^2
$\overline{A}$	surface area of particles, cm^2
A_i	area of individual particle, cm^2
A'	activity, disintegrations/sec
b	annular gap width, cm
B	constant
C	outlet concentration, moles/ml
C_e	surface concentration, moles/ml
C_o	inlet concentration, moles/ml
d	particle diameter, cm
d_i	individual particle diameter, cm
$\mathcal{D}$	molecular mass diffusivity (mass diffusion coefficient), cm^2/sec

Table 2. Summary of Data*

Run No.	Flow Rate (ml/min)	$\bar{V}$ (ml)	$\bar{R}$ (cm)	RPM	(b/r_i)	C/C_o	k (cm/sec)	$\frac{N_{Sh}}{N_{Sc}^{1/3}}$	$(\frac{P}{\bar{V}} \frac{d^4 \rho_L^2}{\mu_L^3})^{1/3}$
65-1	133	3.84	0.0077	2500	0.921	0.102	0.0145	2.31	13.2
65-1A	133	3.84	0.0077	2500	0.921	0.129	0.0115	1.84	13.2
65-2	310	3.84	0.0077	2500	0.921	0.200	0.0142	2.27	13.2
65-2A	309	3.84	0.0077	2500	0.921	0.204	0.0139	2.22	13.2
85-1	302	11.60	0.0077	2500	0.921	0.082	0.0125	2.00	13.3
67-4A	128	21.84	0.0077	2500	0.921	0.019	0.0129	2.06	13.3
67-5	308	21.84	0.0077	2500	0.921	0.036	0.0161	2.57	13.3
67-5A	302	21.84	0.0077	2500	0.921	0.041	0.0138	2.20	13.3
85-2	302	23.12	0.0077	2500	0.921	0.038	0.0143	2.28	13.3
90-1	302	22.0	0.0077	2500	0.921	0.033	0.0178	2.84	13.3
85-3	302	50.08	0.0077	2500	0.921	0.015	0.0164	2.62	13.6
69-8	562	21.84	0.0077	2500	0.921	0.090	0.0111	1.77	13.3
90-2	1024	22.0	0.0077	2500	0.921	0.11	0.0181	2.89	13.3
70-9A	289	66.84	0.0077	2500	0.921	0.008	0.0229	3.66	13.9
74-1	299	66.84	0.0077	2500	0.921	0.008	0.0237	3.78	13.9
74-1A	294	66.84	0.0077	2500	0.921	0.007	0.0277	4.42	13.9
86-4	302	107.68	0.0077	2500	0.921	0.006	0.0208	3.32	13.9
75-2	596	66.84	0.0077	2500	0.921	0.020	0.0191	3.05	13.9
75-2A	611	66.84	0.0077	2500	0.921	0.015	0.0258	4.12	13.9
76-5	309	120.0	0.0077	2500	0.921	0.003	0.0367	5.86	14.0
76-5A	307	120.0	0.0077	2500	0.921	0.005	0.0219	3.50	14.0
77-6	596	120.0	0.0077	2500	0.921	0.005	0.0425	6.79	14.0
77-6A	595	120.0	0.0077	2500	0.921	0.004	0.053	8.46	14.0
68-6	320	21.84	0.0077	1000	0.921	0.057	0.0103	1.65	6.20
68-6A	320	21.84	0.0077	1000	0.921	0.065	0.0090	1.44	6.20
75-3	310	66.84	0.0077	5000	0.921	0.006	0.330	5.27	26.6
75-3A	309	66.84	0.0077	5000	0.921	0.006	0.330	5.27	26.6
76-4	304	66.84	0.0077	7000	0.921	0.008	0.240	3.83	36.7
76-4A	301	66.84	0.0077	7000	0.921	0.008	0.240	3.83	36.7
90-3	1500	66.0	0.0077	2500	0.921	0.032	0.0303	4.84	13.3
91-3A	1500	66.0	0.0077	2500	0.921	0.031	0.0313	5.00	13.3
80-1	312	22.0	0.0040	2500	0.921	0.017	0.0186	1.54	5.6
80-1A	309	22.0	0.0040	2500	0.921	0.017	0.0185	1.52	5.6
83-7	303	22.5	0.015	2500	0.921	0.144	0.0077	2.39	32.2
83-7A	302	22.5	0.015	2500	0.921	0.128	0.0088	2.74	32.3
87-1	598	104.0	0.0077	1000	0.921	0.0060	0.041	6.55	9.2
89-1A	599	104.0	0.0077	1000	0.921	0.0074	0.033	5.27	9.2
87-2	590	104.0	0.0077	2500	0.921	0.0073	0.034	5.43	20.2
89-2A	590	104.0	0.0077	2500	0.921	0.0067	0.037	5.91	20.2
88-3	583	104.0	0.0077	4500	0.921	0.0076	0.032	5.11	33.0
88-3A	611	104.0	0.0077	4500	0.921	0.0070	0.035	5.59	33.0
88-4	585	104.0	0.0077	6000	0.921	0.0073	0.034	5.43	44.0
88-4A	578	104.0	0.0077	6000	0.921	0.0078	0.032	5.11	44.0
92-1	305	22.0	0.0077	2500	3.71	0.047	0.0126	2.01	7.37
92-1A	300	22.0	0.0077	2500	3.71	0.050	0.0117	1.86	7.37
92-2	592	22.0	0.0077	2500	3.71	0.121	0.0095	1.52	7.37
92-3	1022	22.0	0.0077	2500	3.71	0.185	0.0107	1.71	7.37
95-1	284	22.0	0.0077	1000	3.71	0.057	0.0097	1.55	3.10[a]
96-1A	240	22.0	0.0077	1000	3.71	0.055	0.0085	1.36	3.10
96-2	280	22.0	0.0077	2500	3.71	0.042	0.0130	2.08	7.37[b]
96-3	214	22.0	0.0077	4500	3.71	0.028	0.0149	2.38	12.0 [c]
98-1	294	22.0	0.0077	1800	3.71	0.051	0.0112	1.79	4.83
98-2	274	22.0	0.0077	3250	3.71	0.039	0.0137	2.19	8.90
98-3[d]	214	22.0	0.0077	2500	3.71	0.026	0.0160	2.25	18.0
98-4[e]	282	22.0	0.0077	2500	3.71	0.023	0.0238	2.98	23.3
99-9	306	22.0	0.0077	600	0.515	0.041	0.014	2.23	5.95
100-11	304	22.0	0.0077	1500	0.515	0.024	0.024	3.83	12.9
99-8	298	22.0	0.0077	2500	0.515	0.018	0.032	5.11	21.6

*All runs at 25°C unless otherwise noted.

[a]Experimentally determined power per unit volume group = 8.0.

[b]Experimentally determined power per unit volume group = 11.5.

[c]Experimentally determined power per unit volume group = 14.5.

[d]Temperature of run = 40°C.

[e]Temperature of run = 55°C.

D_v	equilibrium distribution coefficient
E_A	activation energy, kcal/mole
f	Fanning friction factor
F	volumetric flow rate, ml/sec
F_o	neutrons/cm^2/sec
F*	correction factor to allow for decay of sample
$\mathcal{F}$	Faraday's constant, coul/g equivalent
g	acceleration of gravity, cm/sec^2
k	mass transfer coefficient, cm/sec
k_c	concentration equilibrium constant
ℓ	length of rotor, cm
n	exponent on the power per unit volume dimensionless group
n_i	number of particles in a given size range, d_i
N	number of atoms of target nuclide
P	power, ergs/sec
r_i	radius of rotor, cm
r_o	radius of cylindrical vessel, cm
R	gas constant, kcal/mole(°K); sulfonic acid group
$\overline{R}$	mean particle radius, cm
R*	radius of spherical shell surrounding particle, cm
S	saturation factor
t	time, sec
$t_{1/2}$	half life, hr
T	absolute temperature, °K
U	velocity, cm/sec
U_i	tangential velocity of inner cylinder, cm/sec

V liquid volume, ml

$\overline{V}$ resin volume, ml

V_{tot} total volume, ml

$\overline{X}$ dimensionless bulk concentration

Z_+, Z_- absolute ion valences for cation and anion

Dimensionless Groups

gravity group: $g\, d^3 \dfrac{(\rho_s - \rho_L)\rho_L}{\mu^2}$

Peclet number: $N_{Pe} = N_{Re}\, N_{Sc} = \dfrac{U\, d}{\mathcal{D}}$

power group: $\dfrac{\frac{P}{V}\, d^4 \rho_L^2}{\mu_L^3}$

Reynolds number: $N_{Re} = \dfrac{\rho d U}{\mu}$

Schmidt number: $N_{Sc} = \dfrac{\mu}{\rho_L \mathcal{D}}$

Sherwood number: $N_{Sh} = \dfrac{kd}{\mathcal{D}}$

Greek Symbols

δ film thickness, cm

λ constant, $0.693/t_{1/2}$, sec^{-1}

$\lambda_+^\circ, \lambda_-^\circ$ limiting ionic conductances for cation and anion, mho/equivalent

μ viscosity, gm/cm-sec

μ_r relative viscosity between suspension and suspending medium

ρ density, gm/cm^3

σ activation cross section for reaction, 4.5×10^{-24} cm^2/atom

τ_i shear stress at the wall of inner cylinder, $dyne/cm^2$

ω speed of rotation, rpm

Subscripts

L liquid

s solid

9.10 Literature References

1. Barker, J.J., and R.E. Treybal, "Mass Transfer Coefficients for Solids Suspended in Agitated Liquids," AIChE J., 6, 289 (1960).

2. Bjorklund, I.S., and W.M. Kays, "Heat Transfer Between Concentric Rotating Cylinders," J. Heat Transfer Trans. ASME, 175 (August 1959).

3. Brian, P.L.T., H.B. Hales, and T.K. Sherwood, "Transport of Heat and Mass Between Liquids and Spherical Particles in an Agitated Tank," AIChE J., 15, 727 (1969).

4. Chandrasekhar, S., "Hydrodynamic and Hydromagnetic Stability," pp. 272-339, Oxford Univ. Press, London (1961).

5. Gandhi, R., and J. Estrin, "Turbulent Momentum Transfer in Two-Phase Cylindrical Couette Flow," AIChE J., 17, 349 (1971).

6. Hales, H.B., "Heat and Mass Transfer from Particles Suspended in a Stirred Tank," Sc.D. Thesis, Dept. of Chem. Eng., Mass. Institute of Technology, Cambridge (1967).

7. Halow, J.S., and G.B. Wills, "Experimental Observations of Sphere Migration in Couette Systems," Ind. Eng. Chem. Fundam., 9(4), 603 (1970).

8. Harriott, P., "Mass Transfer to Particles: Part 1. Suspended in Agitated Tanks," AIChE J., 8, 93 (1962).

9. Helfferich, F., "Ion Exchange," pp. 250-322, McGraw-Hill, New York (1962).

10. Ho, C.Y., J.L. Nardacci, and A.H. Nissan, "Heat Transfer Characteristics of Fluids Moving in a Taylor System of Vortices," AIChE J., 10(2) 194 (1964).

11. Kaye, J., and E.C. Elgar, "Modes of Adiabatic and Diabatic Fluid Flow in an Annulus with an Inner Rotating Cylinder," Trans. ASME, 753 (April 1958).

12. Kays, W.M., "Convective Heat and Mass Transfer," p. 73, McGraw-Hill, New York (1966).

13. Lange, N.A., "Handbook of Chemistry," 10th ed., p. 1680, McGraw-Hill, New York (1967).

14. Lee, D.I., "The Viscosity of Concentrated Suspensions," Trans. Soc. Rheology, 13(2), 273 (1969).

15. Levich, V.G., "Physicochemical Hydrodynamics," pp. 20-24, Prentice-Hall, Englewood Cliffs (1962).

16. Miller, D.N., "Liquid Film Controlled Mass Transfer in Agitated Vessels," Ind. Eng. Chem., 56(10), 18 (1964).

17. Nelson, F., personal communication, ORNL April 6, 1971.

18. Perry, R.H., C.H. Chilton, and S.D. Kirkpatrick, "Perry's Chemical Engineers' Handbook," 4th ed., p. 3-228, McGraw-Hill, New York (1963).

19. Reid, R.C., and T.K. Sherwood, "The Properties of Gases and Liquids," 2nd ed., pp. 561-565, McGraw-Hill, New York (1966).

20. Robinson, R.A., and R.H. Stokes, "Electrolyte Solutions," 2nd ed., p. 317, Butterworth, London (1959).

21. Schlichting, H., "Boundary Layer Theory," 6th ed., pp. 500-503, McGraw-Hill, New York (1968).

22. Selke, W.A., and H. Bliss, "Application of Ion Exchange Copper-Amberlite IR-120 in Fixed Beds," Chem. Eng. Progr., 46, 509 (1950).

23. Sherwood, T.K., and J.M. Ryan, "Mass Transfer to a Turbulent Fluid with and Without Chemical Reaction," Chem. Eng. Sci., 11(2), 81 (1959).

24. Strelow, F.W.E., R. Rethemeyer, and C.J.C. Bothma, "Ion Exchange Selectivity Scales for Cations in Nitric Acid and Sulfuric Acid Media with a Sulfonated Polystyrene Resin," Anal. Chem., 37(1), 106(1965).

25. Sykes, P., and A. Gomezplata, "Particle Liquid Mass Transfer in Stirred Tanks," Canadian J. Chem. Eng., 45, 189 (August 1967).

26. Taylor, G.I., "Fluid Friction Between Rotating Cylinders," Proc. Roy. Soc., A157, 546 (1936).

27. Thomas, D.G., "Transport Characteristics of Suspensions: VIa. A Note on the Viscosity of Newtonian Suspensions of Uniform Spherical Particles," J. Colloid Sci., 20, 267 (1965).

28. "Winning Heavy Metals from Waste Streams," Chem. Eng., 78(9), 62 (1971).

ORNL-MIT-129

INTERNAL

1. L. Dresner
2. G.S. Hill
3. J.S. Johnson, Jr.
4. K.A. Kraus
5. H.A. Mahlman
6. R.E. Minturn
7. G.E. Moore
8. Lewis Nelson
9-10. Fred Nelson
11. J.D. Sheppard
12. A.J. Shor
13. D.G. Thomas
14. D.B. Trauger
15-16. Central Research Library
17. Document Reference Section
18-20. Laboratory Records
21. Laboratory Records, ORNL R.C.
22. ORNL Patent Office
23-37. M.I.T. Practice School

EXTERNAL

38. R.F. Baddour, MIT
39. P.L.T. Brian, MIT
40. L.A. Clomburg, MIT
41. S.M. Fleming, MIT
42. E.R. Gilliland, MIT
43. H.P. Meissner, MIT
44. J.E. Vivian, MIT